Proceedings of the ASME 2015 Dynamic Systems and Control Conference
DSCC2015
October 28-30, 2015, Columbus, Ohio, USA

DSCC2015-9883

A PHENOMENOLOGICAL MODEL FOR PREDICTING THE COMBUSTION PHASING AND VARIABILITY OF SPARK ASSISTED COMPRESSION IGNITION (SACI) ENGINES

Niket Prakash*
Jason B. Martz
Anna G. Stefanopoulou
University of Michigan
Ann Arbor, Michigan 48109
Email: niketpr@umich.edu

ABSTRACT

An advanced combustion mode, Spark Assisted Compression Ignition (SACI) has shown the ability to extend loads relative to Homogenous Charge Compression Ignition (HCCI) combustion but at reduced fuel conversion efficiency. SACI combustion is initiated by a spark, with flame propagation followed by a rapid autoignition of the remaining end-gas fuel fraction. Extending upon previous work [1, 2], the Wiebe function coefficients used to fit the two combustion phases are regressed here as functions of the air path variables and actuator settings. The parameterized regression model enables mean-value modeling and model-based combustion phasing control. SACI combustion however, exhibits high cyclic variability with random characteristics. Thus, combustion phasing feedback control needs to account for the cyclic variability to correctly filter the phasing data. This paper documents the success in regressing the cyclic variability (defined as the standard deviation in combustion phasing) at various operating conditions, again as a function of air path variables and actuator settings. The combination of the regressed mean and standard deviation models is a breakthrough in predicting the mean-value engine behavior and the random statistics of the cycle-to-cycle variability.

*Address all correspondence to this author.

1 INTRODUCTION

While Homogenous Charge Compression Ignition (HCCI) combustion is more fuel efficient than normal spark ignited (SI) combustion, its load range is extremely limited [3–6]. Moreover since the entire combustion process is autoignition based, combustion initiation and phasing are difficult to control. A hybrid SI-HCCI combustion mode, Spark Assisted Compression Ignition (SACI) has shown the ability to extend loads relative to HCCI [7–10]. SACI is a low temperature combustion (LTC) process, combining both spark ignited flame propagation and end-gas autoignition. Beginning with spark-ignition under ultra-dilute conditions, flame and piston compression drive the end-gas to autoignition. Through the appropriate selection of spark timing and temperature at intake valve closing (IVC), which is affected by the temperature of both the hot residual fraction and colder recirculated external exhaust gas, the timing and fraction of SACI end-gas autoignition heat release can be manipulated [8, 11].

The two combustion modes present during SACI occur at distinctly different rates, challenging cycle characterization and control oriented modeling. Yang and Zhu [12] presented a controls oriented SACI model in real time Hardware In the Loop (HIL) simulations. The flame propagation combustion phase was simulated with a two-zone combustion model, while the autoignition phase was simulated with a one-zone model. The transition from flame propagation to autoignition was determined through an Arrhenius integral, calculated at every crank angle de-

gree to predict the start of autoignition. The work in [1] also used an Arrhenius integral to determine the transition point. Glewen et al. [13] used a differentiated form of the double-Wiebe function to build a model that determined the flame propagation to autoignition transition and the relative contribution of each phase during a particular cycle. Real-time analysis was recommended to control the relative contributions to ensure stable combustion.

A simpler predictive-model is proposed in this paper. Given that SACI combustion exhibits high CV, representative cycles [14] from a large SACI dataset are characterized with a double Wiebe function to capture the two-stage SACI heat release with the approach of Hellström et al. [2]. A phenomenological, controls-orientated model is then developed for replicating the heat release profile of SACI combustion. In the future, with such a model, a model-based controller can be created to regulate combustion phasing to an optimum value. An effort was made to build a generalized model that would apply over a range of engine conditions for SACI combustion. Wiebe function durations and exponents were parametrized to mean-value engine variables predicted from cylinder conditions and actuator settings. Combustion phasing or CA 50 (the crank angle location when 50% of the fuel mass has burned) predicted from this model showed good agreement with experimental data.

As with all diluted engines, SACI has cyclic variability which is manifested in the significant fluctuations of cycle to cycle combustion phasing [15]. In contrast with HCCI variability, SACI variability was normally distributed and hence could be represented by a mean and a variance. Therefore, a regression model was also developed to predict the standard deviation of CA 50 for a given steady state operating condition. The model can guide the control design for combustion phasing associated with low fuel consumption, low CV, and low ringing.

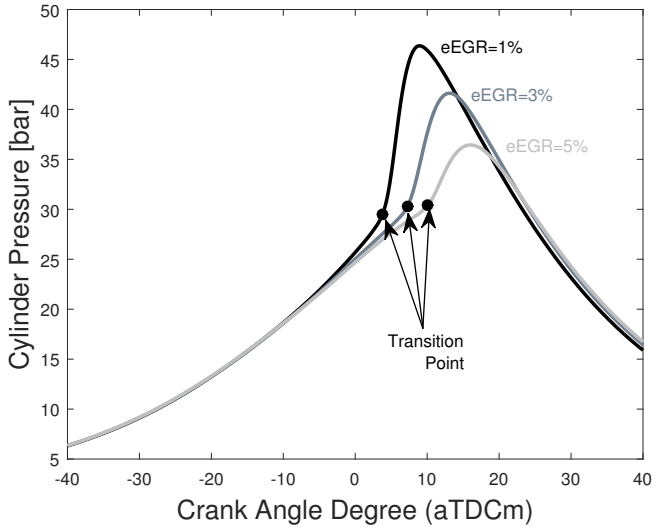

FIGURE 1. CYLINDER PRESSURE FOR DIFFERENT RATES OF EXTERNAL EGR AT THE SAME SPARK AND SOI TIMING SHOW DIFFERENT TRANSITION POINTS TO AUTOIGNITION. SLOW FLAME PROPOGATION UP TO THE TRANSITION POINT IS FOLLOWED BY RAPID AUTOIGNITION. MORE FLAME PROPOGATION LEADS TO LOWER PEAK PRESSURES. SPEED = 1500 RPM, BMEP = 4.2 BAR, SPARK = 40° bTDC, SOI = 400° bTDC, NVO = 154^o

The paper is arranged as follows. Section 2 lists out the experimental set up, the operating conditions and data analysis methods. Section 3 defines the selected pressure cycle from 300 cycles of a steady state data point. Section 4 details the double Wiebe function fitting algorithm. Section 5 describes the regression analysis of the Wiebe function parameters and provides the basis functions. Finally Section 6 highlights SACI cyclic variability and presents predictive models of this variability.

2 EXPERIMENTS AND HEAT RELEASE ANALYSIS

SACI combustion experiments were performed in a prototype modified four-cylinder 2.0 L SI engine, based on the GM Ecotec, running on Tier-II certification gasoline fuel. The compression ratio was 11.7, the bore and stroke were 88 mm, and the connecting rod length was 146 mm. The engine was designed for running multiple modes of combustion such as HCCI, SACI, and SI. The important features of the engine included a dual-lift valvetrain with a dual-independent cam phasers, external exhaust gas recirculation (eEGR), spray-guided direct and port fuel injection, and in-cylinder pressure sensing. Additional details on the prototype engine are provided in [2]. The data presented here are from SACI combustion operated close to stoichiometry, with direct injection, and with low cam lift profiles for intake and exhaust. Negative valve overlap is utilized to trap internal residual gas, while a high-pressure EGR system provides cooled external residual gas.

A total of 264 steady state data points were taken from the engine, each data point consisting of 300 cycles. The load range was from 3.0 bar BMEP to 5.0 bar BMEP and the speed from 1500 RPM to 2000 RPM. Sweeps of spark timing, start of injection timing and external EGR fraction were performed. The spark timing varied from 20° to 65° before top dead center (TDC), while the start of injection timing varied from 340° to 420° before TDC. The in-cylinder external EGR fraction ranged from 1% to 12% and internal EGR fraction from 24% to 50%.

Heat release analysis was performed on the in-cylinder pressure data for each individual cycle from the experiments with the code developed by Larimore et al. [16]. To remove noise prior to heat release analysis, zero-phase filtering was performed on each pressure trace with an eighth order Butterworth filter. The internal residual mass for each cycle was determined with the approach of Fitzgerald et al. [17]. Heat transfer to the combustion chamber boundaries was computed with the modified Woschni [18] method for constant wall temperatures of 473 K.

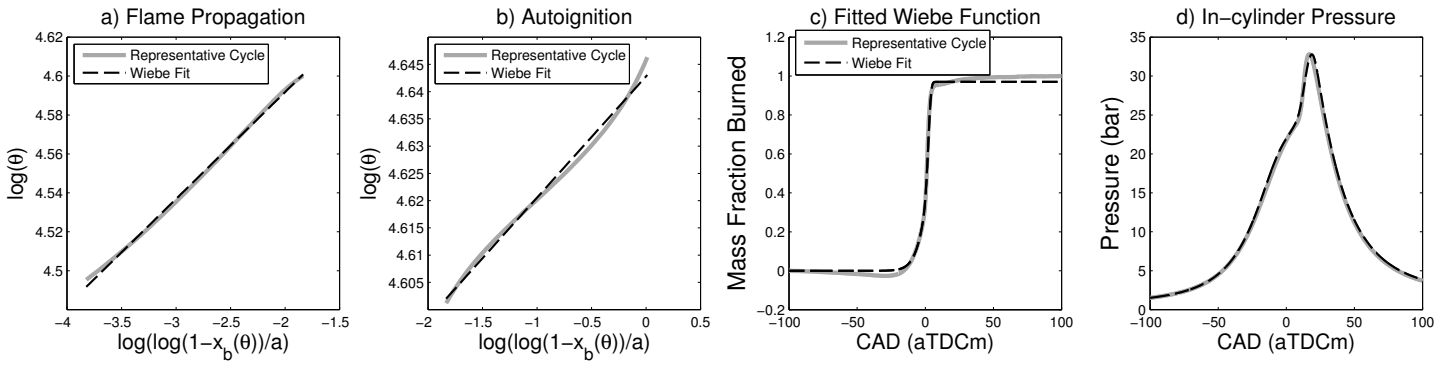

FIGURE 2. FITTED WIEBE FUNCTIONS FOR THE LINEARIZED FLAME PROPOGATION (a) AND AUTOIGNITION (b) COMBUSTION PHASES. THE COMBINED MASS FRACTION BURNED CURVE (c) AND THE FITTED PRESSURE TRACE (d). SPEED = 1500 RPM, BMEP = 3.6 BAR, SPARK = 60° bTDC, SOI = 400° bTDC, NVO = 157°

Heat release analysis was performed in two regions of interest, including windows of the main heat release from 100° before and after TDC, and for the re-compression period of negative valve overlap, from Exhaust Valve Closing to Intake Valve Opening.

3 SELECTION OF THE REPRESENTATIVE CYCLES

Combustion with high rates of internal and external exhaust gas recirculation (EGR) is known to have high cyclic variability (CV). The peak pressure and peak pressure location vary for 300 cycles of a given operating condition. For such high CV at a given speed and load, a range of cycles exist from which the most representative cycle can be found to closely match the mean cycle parameters such as CA 50, the crank angle of 50% mass fraction burned.

Analysis in [14] showed that simply using an ensemble-averaged pressure trace for the heat release analysis produced CA 50 values that were different from the mean CA 50 of all of the cycles processed individually. Hence a representative cycle had to be used that matched the mean CA 50 values. Consistent with [14] the least squares fitted (LSF) mean cycle was the most representative cycle for the mean CA 50. The representative cycle can be defined as the cycle having at a given crank angle, the smallest RMS error in pressure relative to the ensemble averaged pressure trace computed from all cycles. The representative cycles produced the smallest RMS errors in CA 50, combustion duration, maximum pressure, IMEP, internal residual fraction and temperature at IVC, relative to mean values determined for each operating condition within the entire dataset. Although the ensemble average of many cycles is not a useful or representative cycle, the ensemble average of a few cycles can be beneficial for noise reduction.

To this end, the representative cycle is chosen not as a real cycle but instead as the ensemble average of 10 cycles with the smallest RMS error relative to the ensemble averaged pressure data. This is done to reduce the noise in the pressure data and heat release, which poses difficulty for the accurate fitting of the Wiebe functions. This error is then carried into the regression model, compounding it further. Noise also affects computation of the transition point from flame to autoignition combustion, defined as the maxima of the third derivative, which is greatly affected by even the smallest amount of noise. All analyses within this paper were carried out on the representative cycle and the heat release, cylinder composition and thermodynamic parameters generated from these were used in the ensuing regression model.

4 DOUBLE WIEBE FUNCTION FITTING USING A LINEAR LEAST SQUARES APPROACH

The mass fraction burned curves were fit using a double Wiebe function with the linear least squares algorithm of [2, 19]. With this algorithm, combustion is divided into two distinct phases, which is done considering that the transition between the combustion phases shown in Figure 1 is rapid. The transition point is determined from the maxima of the third derivative of the heat release. Wiebe functions for two phases are fit then separately and later joined to form a combined Wiebe function for the entire combustion process through a sigmoid function, with the results of this process shown in Figure 2c.

The Wiebe functions are defined as the mass fraction burned at a crank angle (θ), with three tunable parameters, a, d and m. Parameter a is chosen such that $x(d)$ has a desired value. This is done by assuming 90% mass fraction burned at the end of combustion, or at $x = 0.9$ when $\theta = d$ and $a = log(1-0.90) = -2.3026$. Parameter d is the duration of combustion and m the exponent. The Wiebe function is fit to the mass fraction burned curve in the crank angle duration from 5% to 90% of mass fraction burned. The exponential Wiebe function is linearized to give the other two unknown parameters d and m as the slope and in-

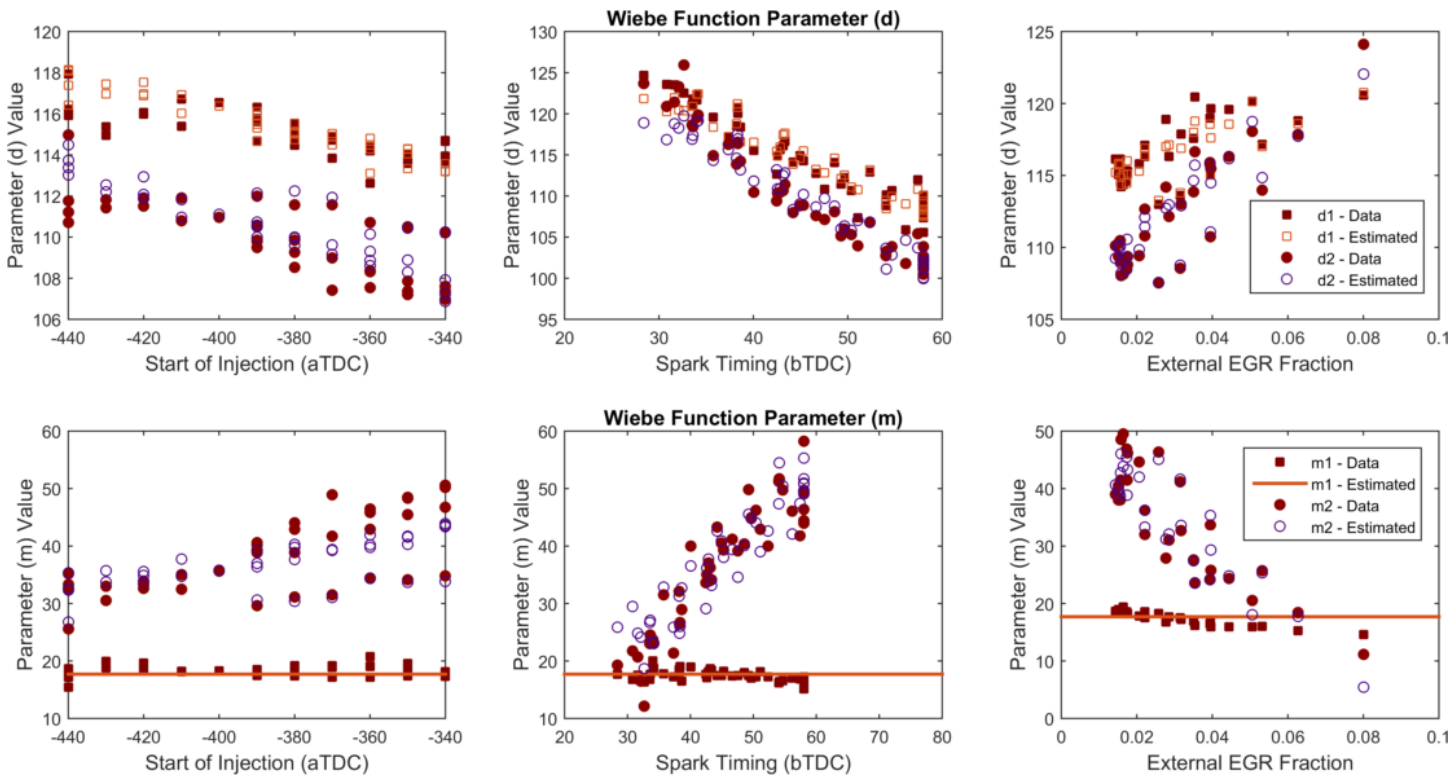

FIGURE 3. WIEBE FUNCTION PARAMETERS 'D' AND 'M' FOR THE SPARK IGNITION AND AUTOIGNITION PHASES OF COMBUSTION. TRENDS OF D1 AND D2 FOLLOW EACH OTHER. PARAMETER M1 IS ALMOST CONSTANT AND M2 VARIES SIGNIFICANTLY

tercept respectively:

$$x(\theta;m,d) = 1 - exp[a(\frac{\theta}{d})^{(m+1)}] \longrightarrow$$
$$log\theta = \frac{1}{m+1} log[\frac{1}{a} log(1-x(\theta))] + log(d) \quad (1)$$

There are several methods to determine the start and end of combustion in the literature. They include using the negative most point and the positive most point of the crank angle resolved heat release curve as the start and end respectively [2]; using the range of crank angle degrees where the heat release rate is positive [13], or using the spark timing as the start of combustion [20]. In the current work, using such methods degraded the ability of the computed Wiebe functions to accurately reproduce the experimental results. Therefore, the mass fraction burned data was considered for a window from a 100^o CA before and after TDC combustion, normalized over this range and then fit for a given span of mass fraction burned. This provided the added benefit of eliminating the need to find and regress the starting and end points for combustion.

As shown in Figure 2, the Wiebe functions are well fit for the spark ignition region and also through most of the autoignition phase. The main source of error is towards $90-95\%$ mass fraction burned, where the Wiebe function is unable to accurately model the gradual drop in the heat release rate. When the burn duration under consideration was increased above 90%, the Wiebe function showed a greater error in the $10-90\%$ burn region. This implied that 90% is the optimum burn duration to consider for the fitting algorithm under the current conditions. By using a range up to 90% MFB and then extrapolating over the rest of the crank angle degrees, the Wiebe functions do not reach 100% MFB. However, such a fitting range ensured that the error between the model and experimental CA 50 was minimized.

5 WIEBE FUNCTION REGRESSION

The variation in the Wiebe function parameters d and m are shown in Figure 3 for sweeps of SOI timing, spark timing and varying rates of external EGR. These parameters were fit with a least squares approach that minimized predicted RMS errors relative to experimental values. Parameter $d1$ (defined for the flame based Wiebe function) varies from 105 to 125 and $d2$ (for the second autoignition Wiebe function) from 100 to 126. Parameter $m1$, the slope for the flame based combustion, is approximately constant, and is held constant for the regression analysis. Parameter $m2$ is highly variable, as the rate of autoignition during SACI

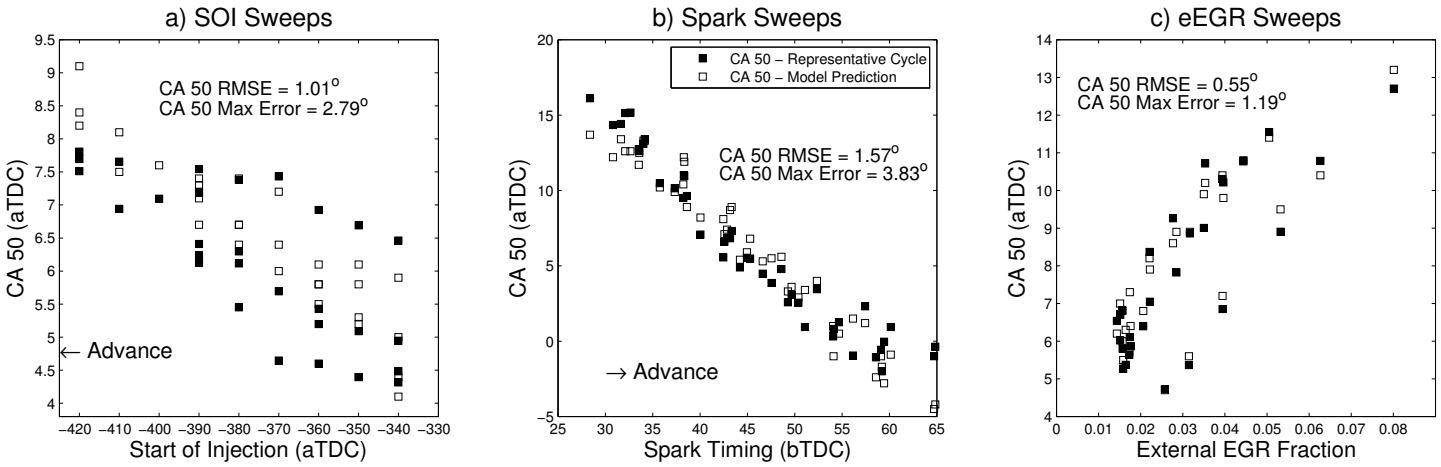

FIGURE 4. MEASURED AND PREDICTED CA 50 OVER ACTUATOR SWEEPS OF a) START OF INJECTION TIMING, b) SPARK TIMING AND c) EXTERNAL EGR FRACTION

depends on operating strategy [9] and hence was parameterized.

Variables chosen for the global regression were, spark timing (*Spark*), SOI timing (*SOI*), external EGR fraction (*eEGR*), and the fuel to charge equivalence ratio (ϕ') [21], which can be used as an estimate of the level of charge dilution within the cylinder

$$\phi' = (1-(eEGR+iEGR))/\lambda. \tag{2}$$

Variable *iEGR* is the fraction of the internal residual relative to the total mass within the cylinder and λ the ratio of actual air-fuel ratio to stoichiometric air-fuel ratio.

The data set under analysis consisted of sweeps of spark timing, start of injection timing and external EGR fraction over different loads as shown in Figure 4. It was found that CA 50 varies inversely with spark and SOI timings and proportionately with eEGR. Regression models using linear least squares were created for individual sweeps to determine the engine parameters affecting the Wiebe function and their orders. The basis function was used to construct a global regression model that could be applied over all actuator sweeps and all loads.

It was found that the Wiebe function parameter $d2$ showed a good linear correlation with CA 50. Hence $d2$ became the most important parameter to be regressed for accurate prediction of CA 50. In particular, $d2$ was found to be inversely related to spark timing and start of injection timing, and varied proportionately to the external EGR fraction in the cylinder. The cylinder composition (quantified via ϕ') also affected $d2$. The variables α_i, β_i and γ_i are the regression coefficients. The resulting expression of $d2$ is as follows:

$$\begin{aligned} d2 = \alpha_1 + \alpha_2 \cdot SOI + \alpha_3 \cdot eEGR + \alpha_4 \cdot Spark \\ + \alpha_5 \cdot SOI \cdot eEGR + \alpha_6 \cdot \phi'. \end{aligned} \tag{3}$$

Parameter $d1$ follows the trends of parameter $d2$ and its expression is given in equation 4. The ratio of flame to autoignition heat release is determined by the transition point, which is dictated by the exponents $m1$ and $m2$. As mentioned above, $m1$ is held constant, while $m2$ varies significantly over the different operating conditions and is a function of charge dilution (i.e. ϕ' and external EGR fraction). $m2$ was also found to be a function of parameter $d2$ due to the fact that $d2$ captures the effect of actuator timings in its computation:

$$d1 = \beta_1 + \beta_2 \cdot eEGR + \beta_3 \cdot d2 \tag{4}$$

$$m2 = \gamma_1 + \gamma_2 \cdot eEGR + \gamma_3 \cdot \phi'. \tag{5}$$

Although the regression model does not contain any explicit speed correlation, it was still able to capture CA 50 in the range of 1500 to 2000 RPM. A more drastic increase of enigne speeds would lead to changes in the flame wrinkling and possibly combustion characteristics, which may require another parametrization to account for such changes.

The RMS error for CA 50 predicted by the Wiebe function regression models was 1.2° CA over all data points with a mean absolute error of 0.9° CA. The highest under-prediction in CA 50 was 2.8^o CA, while the the highest over prediction was 3.8° CA. The Wiebe function parameters and associated prediction accuracy are shown in Figure 4.

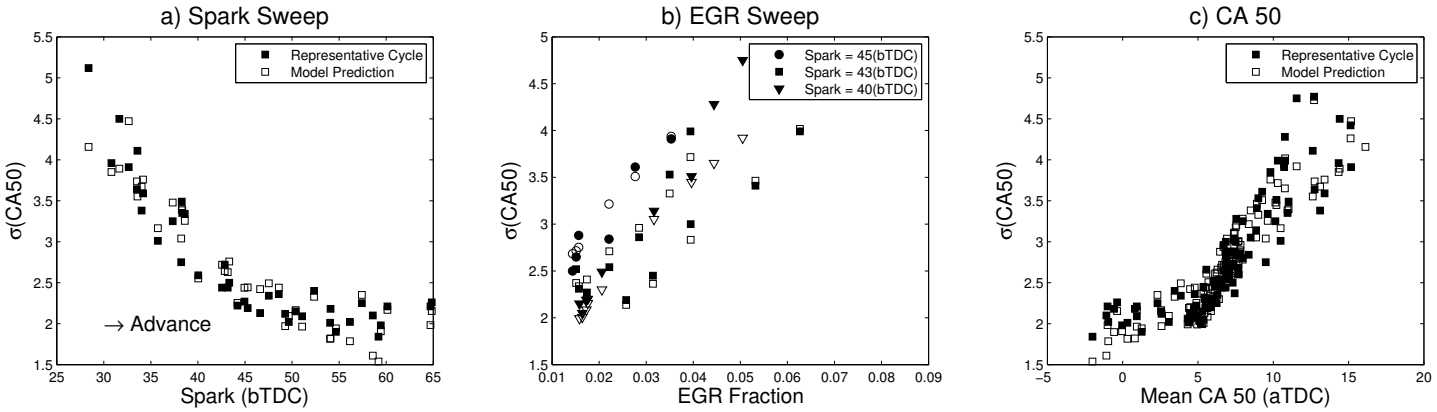

FIGURE 5. STANDARD DEVIATION OF CA 50 AGAINST SWEEPS OF a) SPARK TIMING, b) EXTERNAL EGR AND c) MEAN COMBUSTION PHASING

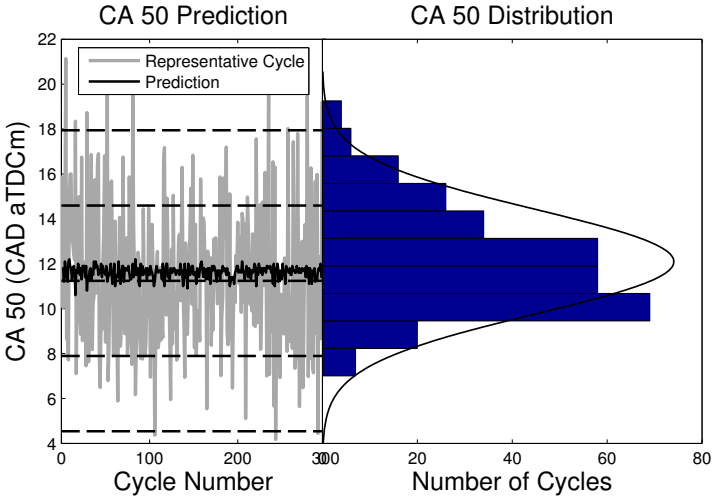

FIGURE 6. CYCLIC VARIABILITY IN HEAT RELEASE OF 300 CYCLES FOR A STEADY STATE DATA POINT WITH MEAN, $\pm\sigma$ AND $\pm 2\sigma$ LINES. SPEED =1500 RPM, BMEP =3.7 BAR, SPARK = 38° bTDC, SOI =400° bTDC, NVO =161^o

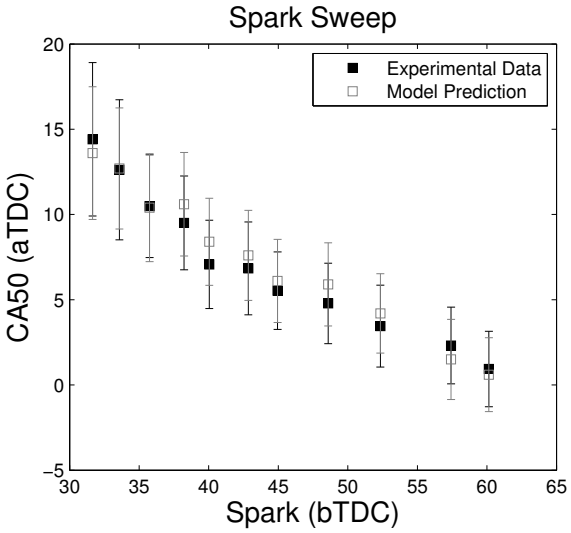

FIGURE 7. PREDICTION OF CA 50 AND STANDARD DEVIATION OF CA 50 FOR STEADY STATE SPARK SWEEPS

6 CYCLIC VARIABILITY INVESTIGATION

The data set considered here had a range of 2° to 5° CA standard deviation in CA 50 corresponding to a 1% to 5% IMEP COV. This variation could be caused by multiple factors such as differences in the amount of hot residual mass trapped from the previous cycle that would influence the temperature at the time of spark and transition to autoignition [22]. Additionally, bulk and turbulent flow fluctuations can affect flame stretch hence the duration of flame based combustion [23].

Steady state data points were processed cycle-by-cycle and the trapped internal residual mass was determined cyclically. An iterative form of the Fitzgerald algorithm was used for each case where the individual cycle pressure trace and an average exhaust gas temperature were inputs to the algorithm. Heat release analysis was also performed iteratively on each pressure trace individually. From cyclic analysis of the pressure traces for a given steady state operating condition, a wide variation was observed in combustion phasing and combustion duration. The gross heat release and maximum pressure varied from 530 J to 600 J and 23 bar to 44 bar, respectively. Internal EGR also varied from 38% to 45%, leading to a variation in ϕ' of 0.53 to 0.60. The temperature at intake valve closing was positively correlated with ϕ'. Similar deviations were observed for other operating conditions.

For the Wiebe function model described above, the only input changing cycle by cycle was ϕ'. Imposing these variations onto the Wiebe regression model for each cycle, CA 50 was predicted to be nearly constant as shown in Figure 6. An experi-

mental standard deviation in CA 50 of 3.35° CA was observed, while the Wiebe regression model predicted a standard deviation of 0.28° CA, with phasing close to the mean. The mean prediction is expected as the model was created on a representative cycle that was closest to the mean CA 50 value. However, the lack of variability in the CA 50 predicted by the model, especially for such large variations in ϕ', suggests that something other than the cylinder composition and associated fluctuations in IVC temperature contributes to the cyclic variability. To this end an effort was made to regress the variation in CA 50, quantified with the CA 50 standard deviation ($\sigma(CA50)$) to various engine conditions and actuator settings.

Interestingly, the statistics of the CA 50 variation were well correlated to spark advance, cylinder composition and combustion phasing. It was found that an advanced spark reduced σ(CA 50), as shown in Figure 5a. As expected the rate of external exhaust gas recirculation (eEGR) also influenced the variability in a linear fashion, with variability increasing with increasing eEGR fraction as shown in Figure 5b. Another influence on the standard deviation was the mean combustion phasing itself. A linear relation was observed showing that if the steady state data point had a later CA 50 it produced more variability in phasing as shown in Figure 5c.

The cold external charge influences the variability by reducing the temperature at the time of spark, delaying the transition to autoignition and, hence making the flame more susceptible to cylinder composition and turbulence. This model could provide a useful method to arrive at an optimum EGR rate which would not significantly increase the fluctuations of CA 50 while at the same time satisfying ideal operating conditions for high efficiency operation.

A combination of spark timing, eEGR and mean CA 50 were used to create a regression model to predict the standard deviation of CA 50. The prediction for CA 50 (markers) and cyclic variability (error bars) can be seen in Figure 7 with the regression in Equation 6:

$$\sigma(CA50) = \delta_1 + \delta_2 \times Spark + \delta_3 \times eEGR + \delta_4 \times CA50. \quad (6)$$

Model predictions followed the general trend of the data and showed an RMS error of 0.24^o. Prediction of the standard deviation can be used in determining appropriate actuator settings for low variability regions and with appropriate combustion phasing. However, care must be taken to ensure that the regions of low variability, i.e. early CA 50 are not so early that the pressure rise rates are sufficiently high enough to cause ringing. Ringing intensity was calculated by Equation 7 [24], where MPRR is the maximum pressure rise rate and MaxP the maximum pressure during the cycle:

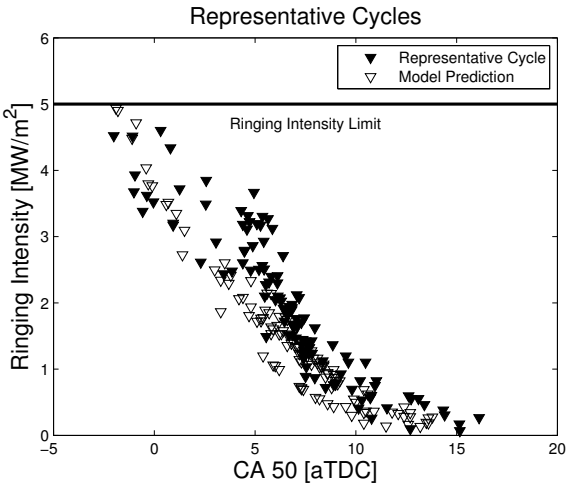

FIGURE 8. PREDICTION OF RINGING INTENSITY OF REPRESENTATIVE CYCLES. THE PREDICTIONS HAVE RMSE = 0.78 RELATIVE TO THE EXPERIMENTS

$$RI = 2.88 \times 10^{-8} \times (MPRR) \times (Speed)^2/(MaxP). \quad (7)$$

By using the Wiebe function to calculate the pressure over the given crank angle range, the maximum pressure and maximum pressure rise rates were computed by the model. The results are shown in Figure 8. Hence the combustion phasing has to be kept later than the CA 50s associated with elevated ringing yet before the late CA 50s associated with the high CV region.

7 CONCLUSIONS

A phenomenological, controls-oriented predictive model was devised to characterize SACI combustion and to predict combustion phasing (CA 50). The model was based on a double Wiebe function and predicted the Wiebe function parmeters $d1$, $d2$ and $m2$, for actuator settings of spark timing, SOI timing and charge composition through external EGR fraction and ϕ'. The model predicted a mean behavior of combustion phasing given the above variables.

For quantification of cyclic variability, another regression model was created to predict the standard deviation of CA 50. Use of this model could determine the operating conditions for low variability and act as a filter while driving the above model. It was also shown that while regions of early CA 50 corresponded to low variability, they also corresponded to high pressure rise rates. Representative cycles close to the ringing limit had several cycles above the limit and hence care should be taken to ensure that regions of high ringing are not approached.

ACKNOWLEDGMENT

This material is based upon work supported partially by the Department of Energy [National Energy Technology Laboratory] under Award Number(s) DE-EE0003533 and partially funded by Robert Bosch LLC. The authors would like to thank Dr. Shyam Jade for the SACI data.

REFERENCES

[1] Qu, Z., Ravi, N., Oudart, J., Doran, E., Mittal, V., and Kojic, A. "Control-oriented modeling of spark assisted compression ignition using a double wiebe function". In ACC, no. (Accepted).

[2] Hellström, E., Stefanopoulou, A., and Jiang, L., 2013. "A linear least-squares algorithm for double-wiebe functions applied to spark-assisted compression ignition". *Journal of Engineering for Gas Turbines and Power,* ***136***.

[3] Najt, P. M., and Foster, D. E., 1983. "Compression-ignited homogeneous charge combustion". In SAE, no. 830264.

[4] Thring, R. H., 1989. "Homogeneous-charge compression-ignition (HCCI) engines". In SAE, no. 892068.

[5] Li, J., H., Z., and Ladommatos, N., 2001. "Research and development of controlled autoignition (CAI) combustion in a 4-stroke multi-cylinder gasoline engine". In SAE, no. 2001-01-3608.

[6] Aoyama, T., Hattori, Y., and Mizuta, J., 1996. "An experimental study on premixed-charge compression ignition gasoline engine". In SAE, no. 960081.

[7] Saxena, S. Bedoya, I., 2013. "Fundamental phenomena affecting low temperature combustion and hcci engines, high load limits and strategies for extending these limits". *Progress in Energy and Combustion Science,* ***39***, pp. 457–488.

[8] Yun, H., Wermuth, N., and Najt, P., 2010. "Extending the high load operating limit of a naturally-aspirated gasoline hcci combustion engine". *SAE Int J Engines,* ***3(1)***, p. 681699.

[9] Manofsky, D., Vavra, J., Assanis, D., and Babjimopoulou, A., 2011. "Bridging the gap between HCCI and SI: Spark-assisted compression ignition". In SAE, no. 2011-01-1179.

[10] Szybist, J., Nafziger, E., and Weall, A., 2010. "Load expansion of stoichiometric hcci using spark assist and hydraulic valve actuation". *SAE Int J Engines,* ***3(2)***, pp. 244–258.

[11] Olesky, L., Martz, J., Lavoie, G., Vavra, J., Assanis, D., and Babajimopoulos, A., 2013. "The effects of spark timing, unburned gas temperature, and negative valve overlap on the rates of stoichiometric spark assisted compression ignition combustion". *Appl Energy,* ***2013***, pp. 407–417.

[12] Yang, X., and Zhu, G. G., 2012. "A control-oriented hybrid combustion model of a homogeneous charge compression ignition capable spark ignition engine". *Proc IMechE,* ***226***, pp. 1380–1395.

[13] Glewen, W. J., Wagner, R. M., Edwards, K. D., and Daw, C. S., 2009. "Analysis of cyclic variability in spark-assisted HCCI combustion using a double wiebe function". *Proc Combustion Institute,* ***32***, pp. 2885–2892.

[14] Temel, V., and Sterniak, J., 2014. "Characterization of SACI combustion for use in model based controls". In SAE, no. 2014-01-1289.

[15] Young, M. B., 1980. "Cyclic dispersion - some quantitative cause-and-effect relationships". In SAE, no. 800459.

[16] Larimore, J., Hellström, E., Li, J., and Stefanopoulou, A., 2012. "Experiments and analysis of high cyclic variability at the operational limits of spark-assisted HCCI combustion". In ACC, pp. 2072–2077.

[17] Fitzgerald, R., Steeper, R., Snyder, J., Hanson, R., and Hessel, R., 2010. "Determination of cycle temperatures and residual gas fraction for HCCI negative valve overlap operation". In SAE, no. 2010-01-0343.

[18] Hohenberg, G. F., 1979. "Advanced approaches for heat transfer calculations". In SAE, no. 790825.

[19] Ghojel, J., 2010. "Review of the development and applications of the wiebe function: a tribute to the contribution of ivan wiebe to engine research". *International Journal of Engine Research,* ***11***, pp. 297–312.

[20] Rousseau, S., Lemoult, B., and Tazerout, M., 2009. "Combustion characterization of natural gas in a lean burn spark-ignition engine". *Proc IMechE,* ***32***, pp. 2885–2892.

[21] Lavoie, G., Martz, J., Wooldridge, M., and Assanis, D., 2010. "A multi-mode combustion diagram for spark assisted compression ignition". *Combust. Flame,* ***157***, pp. 1106–1110.

[22] Larimore J. Hellström, E., Sterniak, J., Jiang, L., and Stefanopoulou, A., 2012. "Quantifying cyclic variability in a multicylinder HCCI engine with high residuals". *Journal of Engineering for Gas Turbines and Power,* ***134***.

[23] Dai, W., Trigui, N., and Lu, Y., 2000. "Modeling of cyclic variations in spark-ignited engines". In SAE, no. 2000-01-2036.

[24] Polovina, D., McKenna, D., Wheeler, J., Sterniak, J., Miersch-Wiemers, O., Mond, A., and Yilmaz, H., 2013. "Steady-state combustion development of a downsized multi-cylinder engine with range extended HCCI/SACI capability". In SAE, no. 2013-01-1655.